SLAC-PUB-14698

34th International Conference on High Energy Physics (ICHEP08). Philadelphia, PA (USA), Jul 30-Aug 5, 2008.

Angular and Rate Asymmetries in the Decays $B \to K^{(*)}\ell^+\ell^-$

Kevin T. Flood, on behalf of the *BABAR* Collaboration
University of Wisconsin, Madison, WI 53706, USA

We use a sample of 384 million $B\overline{B}$ decays collected with the *BABAR* detector at the PEP-II asymmetric e^+e^- storage ring to study the flavor-changing neutral current decays $B \to K^{(*)}\ell^+\ell^-$, where $\ell^+\ell^-$ is either e^+e^- or $\mu^+\mu^-$. We present measurements in two dilepton mass bins, one below the J/ψ resonance and the other above, of the lepton forward-backward asymmetry $\mathcal{A}_{FB}$ and the longitudinal K^* polarization F_L in $B \to K^*\ell^+\ell^-$, along with isospin rate asymmetries in $B \to K^*\ell^+\ell^-$ and $B \to K\ell^+\ell^-$ final states.

The decays $B \to K^{(*)}\ell^+\ell^-$, where $\ell^+\ell^-$ is either e^+e^- or $\mu^+\mu^-$, arise from flavor-changing neutral current processes that are forbidden at tree level in the Standard Model (SM). The lowest-order SM processes contributing to these decays are the photon penguin, Z penguin and W^+W^- box diagrams. Their amplitudes are expressed in terms of hadronic form factors and effective Wilson coefficients C_7, C_9 and C_{10}, representing the electromagnetic penguin diagram, and the vector part and the axial-vector part of the Z penguin and W^+W^- box diagrams, respectively [1]. New physics contributions may enter the penguin and box diagrams at the same order as the SM diagrams [2]. We present measurements of the lepton forward-backward asymmetry $\mathcal{A}_{FB}$ and longitudinal K^* polarization F_L in $B \to K^*\ell^+\ell^-$, along with isospin rate asymmetries in $B \to K^*\ell^+\ell^-$ and $B \to K\ell^+\ell^-$ final states, in two bins of dilepton mass squared $q^2 = m^2_{\ell^+\ell^-}$, one below the J/ψ resonance and the other above. Sensitive indirect searches for new physics effects using these observables [3] are possible as hadronic uncertainties in calculations are expected to cancel [4]. *BABAR* results on branching fractions, direct *CP* and lepton-flavor asymmetries, $\mathcal{A}_{FB}$ and F_L have been previously published, however, only a limit for $\mathcal{A}_{FB}$ in the low q^2 region was established [5].

The *CP*-averaged isospin asymmetry

$$A_I^{K^{(*)}} \equiv \frac{\mathcal{B}(B^0 \to K^{(*)0}\ell^+\ell^-) - r\mathcal{B}(B^\pm \to K^{(*)\pm}\ell^+\ell^-)}{\mathcal{B}(B^0 \to K^{(*)0}\ell^+\ell^-) + r\mathcal{B}(B^\pm \to K^{(*)\pm}\ell^+\ell^-)} \tag{1}$$

where $r = \tau_0/\tau_+ = 1/(1.07 \pm 0.01)$ is the ratio of the B^0 and B^+ lifetimes [6], has a SM expectation of $+6-13\%$ as $q^2 \to 0$ for $B \to K^*\ell^+\ell^-$ [7]. This is consistent with the measured asymmetry of $3\pm3\%$ in $B \to K^*\gamma$ [6]. A calculation of the predicted K^{*+} and K^{*0} SM rates integrated over the low q^2 region gives $A_I^{K^*} = -0.00^{+0.005}_{-0.006}$ [8, 9]. Given that the expected SM isospin asymmetry arises from pure photon penguin contributions to $B \to K^*\ell^+\ell^-$, there is no expectation of such an asymmetry in $K\ell^+\ell^-$. In the high q^2 region, although there may be possible contributions from higher charmonium resonances, the measured asymmetry in $J/\psi\,K^{(*)}$ is only a few percent [6], and any SM $A_I^{K^*}$ can be reasonably expected to be similarly insignificant. We measure isospin asymmetries in a low q^2 region $0.1 < q^2 < 7.02\,\mathrm{GeV}^2/c^4$, and a high region $q^2 > 10.24\,\mathrm{GeV}^2/c^4$, where any likely contributions from J/ψ and $\psi(2S)$ have been removed by vetoing events $7.02 < q^2 < 10.24\,\mathrm{GeV}^2/c^4$ and $12.96 < q^2 < 14.06\,\mathrm{GeV}^2/c^4$, respectively.

The K^* longitudinal polarization fraction F_L can be determined from the distribution of the angle $\cos\theta_K$ between the K and the B directions in the K^* rest frame using a fit to $\cos\theta_K$ of the form [10]

$$\frac{3}{2}F_L\cos^2\theta_K + \frac{3}{4}(1-F_L)(1-\cos^2\theta_K) \tag{2}$$

Likewise, the lepton forward-backward asymmetry $\mathcal{A}_{FB}$ can be determined from the distribution of the angle $\cos\theta_\ell$ between the $\ell^+(\ell^-)$ and the $B(\overline{B})$ direction in the $\ell^+\ell^-$ rest frame using a fit to $\cos\theta_\ell$ of the form [10]

$$\frac{3}{4}F_L(1-\cos^2\theta_\ell) + \frac{3}{8}(1-F_L)(1+\cos^2\theta_\ell) + \mathcal{A}_{FB}\cos\theta_\ell \tag{3}$$

These angular measurements are also done in low and high q^2 regions, with the low region slightly more narrowly defined than above, $0.1 < q^2 < 6.25\,\mathrm{GeV}^2/c^4$, in order to absolutely remove any possible contributions from J/ψ and

Work supported in part by US Department of Energy contract DE-AC02-76SF00515.

$\psi(2S)$ decays, which have a distinct angular structure but are otherwise indistinguishable from signal decays. As shown in Eq. 3, an experimental determination of F_L is required to obtain a model-independent $\mathcal{A}_{FB}$ result.

Variations in F_L and $\mathcal{A}_{FB}$ as a function of q^2 result from interference among the different amplitudes. The expected SM behavior of F_L and $\mathcal{A}_{FB}$, along with variations due to non-SM opposite-sign Wilson coefficients, is shown by the curves in Fig. 1. At low q^2, where C_7 dominates, $\mathcal{A}_{FB}$ is expected to be small with a zero-crossing point at $q^2 \sim 4\,\mathrm{GeV}^2/c^4$ [11, 12, 13]. An experimental constraint on the magnitude of C_7 comes from the measured inclusive branching fraction for $b \to s\gamma$ [6, 13, 14], which corresponds to the limit $q^2 \to 0$, but its sign is unknown. At high q^2 in the SM, the product C_9C_{10} is expected to give a large positive asymmetry. Right-handed weak currents would have an opposite-sign C_9C_{10}, leading to a negative $\mathcal{A}_{FB}$ contribution at high q^2. Contributions from other non-SM processes could change the magnitudes and relative signs of C_7, C_9 and C_{10}, and introduce complex phases between them [10, 15].

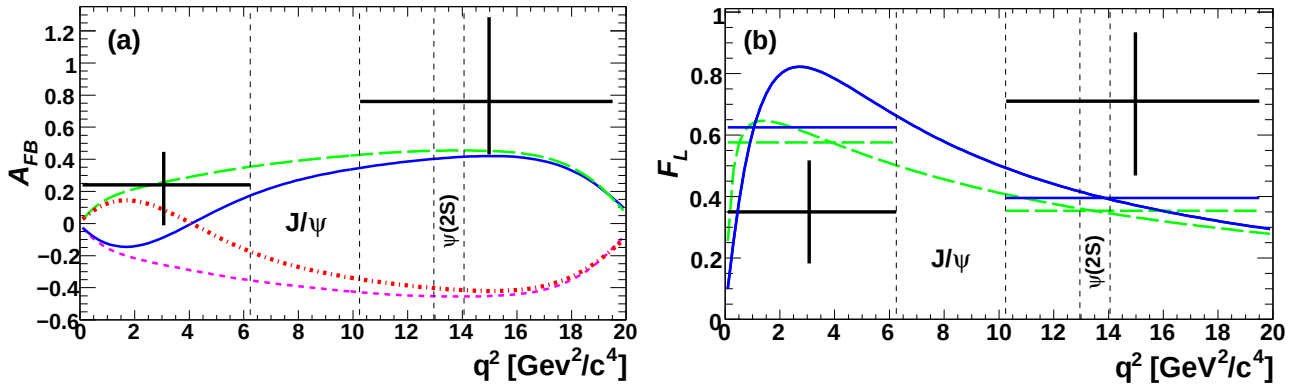

Figure 1: (a) $\mathcal{A}_{FB}$ and (b) F_L results showing comparisons with SM (solid), $C_7 = -C_7^{SM}$ (long dash), $C_9C_{10} = -C_9^{SM}C_{10}^{SM}$ (short dash), $C_7 = -C_7^{SM}, C_9C_{10} = -C_9^{SM}C_{10}^{SM}$ (dash-dot). Statistical and systematic errors are added in quadrature. Expected F_L values integrated over each q^2 region are also shown. The F_L curves with $C_9C_{10} = -C_9^{SM}C_{10}^{SM}$ are nearly identical to the two curves shown.

We use a data sample of 384 million $B\overline{B}$ pairs collected at the $\Upsilon(4S)$ resonance with the *BABAR* detector [16] at the PEP-II asymmetric-energy e^+e^- collider at SLAC. Tracking is provided by a five-layer silicon vertex tracker (SVT) and a 40-layer drift chamber (DCH) in a 1.5-T magnetic field. We identify electrons with a CsI(Tl) electromagnetic calorimeter, and muons using an instrumented magnetic flux return. Electrons (muons) are required to have momenta $p > 0.3(0.7)\,\mathrm{GeV}/c$ in the laboratory frame. We combine photons with electrons when they are consistent with bremsstrahlung, and do not use electrons that are associated with a photon converting to a low-mass e^+e^- pair. We identify K^+ using a detector of internally reflected Cherenkov light, as well as ionization energy loss measurements from the DCH and SVT. Charged tracks other than identified e, μ and K candidates are treated as pions. Neutral pion candidates are formed from two photons with laboratory energies $E_\gamma > 50\,\mathrm{MeV}$ and an invariant mass between 115 and 155 MeV/c^2.

We reconstruct signal events in ten separate final states containing an e^+e^- or $\mu^+\mu^-$ pair, and a $K_S^0(\to \pi^+\pi^-)$, K^+, or $K^*(892)$ candidate with an invariant mass $0.82 < M(K\pi) < 0.97\,\mathrm{GeV}/c^2$. We reconstruct K^{*0} candidates in the final state $K^+\pi^-$, and K^{*+} candidates in the final states $K^+\pi^0$ and $K_S^0\pi^+$ (charge conjugation is implied throughout). Neutral $K_S^0 \to \pi^+\pi^-$ candidates are required to have an invariant mass consistent with the nominal K^0 mass [17], and a flight distance from the primary interaction point which is more than three times its uncertainty. We also study final states $K^{(*)}h^\pm\mu^\mp$, where h is a track with no particle identification (PID) requirement applied, to characterize backgrounds from hadrons misidentified as muons. Signal decays are characterized using the kinematic variables $m_{\rm ES} = \sqrt{s/4 - p_B^{*2}}$ and $\Delta E = E_B^* - \sqrt{s}/2$, where p_B^* and E_B^* are the B momentum and energy in the $\Upsilon(4S)$ center-of-mass (CM) frame, and $\sqrt{s}$ is the total CM energy. We define a fit region $m_{\rm ES} > 5.2\,\mathrm{GeV}/c^2$, with $-0.07 < \Delta E < 0.04$ $(-0.04 < \Delta E < 0.04)$ GeV for e^+e^- $(\mu^+\mu^-)$ final states in the low q^2 region, and $-0.08 < \Delta E < 0.05$ $(-0.05 < \Delta E < 0.05)$ GeV for high q^2.

The main backgrounds arise from random combinations of leptons from semileptonic B and D decays, which are suppressed using event shape variables, vertexing information and missing energy combined in event selection neural networks (NNs). We use simulated samples of signal and background events in the construction of the NNs and, assuming rates consistent with accepted values [6], we optimize the NN selections for best statistical significance in the number of expected signal events in our dataset. A further background contribution comes from $B \to D(\to K^{(*)}\pi)\pi$ decays where both pions are misidentified as leptons. This background is significant only in dimuon final states, as the pion misidentification rate for electrons is $< 0.1\%$. We veto these events by assigning the pion mass to a muon candidate and requiring that the invariant mass of the hypothetical $K^{(*)}\pi$ system be outside the range 1.84-1.90 GeV/c^2. We perform blind fits for both the isospin and angular observables, in which all event selection criteria were determined prior to examining events in the fit region.

We directly fit the data with $A_I^{K^{(*)}}$ as a floating parameter using a simultaneous unbinned maximum likelihood $m_{\rm ES}$ fit across all modes contributing to a particular A_I measurement. An ARGUS shape [18] with floating shape parameter and normalization is used to describe combinatorial background. For the signal, we use a fixed Gaussian shape unique to each final state, with mean and width determined from fits to the analogous final states in the large samples of vetoed $J/\psi K^{(*)}$ events. Events with misidentified muons escaping the D mass veto are accounted for using $K^{(*)}h^{\pm}\mu^{\mp}$ events weighted by the per-particle probability, determined from uncorrelated PID control samples, for $h^{\pm}$ to be misidentified. We also account for small contributions from misreconstructed signal events and charmonium events that escape the charmonium mass vetos. We test the fit using the large samples of vetoed $J/\psi K^{(*)}$ and $\psi(2S)K^{(*)}$ events, and find good agreement with accepted values for branching fractions to the individual final states used here and the small charmonium isospin asymmetries [17].

We consider systematic uncertainties associated with reconstruction efficiencies; hadronic background parameterization in di-muon final states; peaking background contributions obtained from simulated events; and possible isospin asymmetries in the background pdfs. We quantify efficiency-related systematics using the vetoed $J/\psi\, K^{(*)}$ samples, including charged track, π^0, and K^0_S reconstruction, PID, NN selection, and the ΔE and K^* mass selections. Nearly all systematic effects largely cancel in the A_I ratio, and the final systematic uncertainties are small compared to the statistical ones.

Table I shows the $A_I^{K^{(*)}}$ results. We find no significant isospin asymmetries in the high q^2 region, but we find evidence for large negative asymmetries in the low region. We calculate the statistical significance with which a null isospin asymmetry hypothesis is rejected using the change in log likelihood $\sqrt{2\Delta \ln \mathcal{L}}$ between the nominal fit to the data and a fit with $A_I^{K^{(*)}} = 0$ fixed. Figure 2 shows the likelihood curves obtained from the $K\ell^+\ell^-$ and $K^*\ell^+\ell^-$ fits. The parabolic nature of the curves in the $A_I^{K^{(*)}} > -1$ region demonstrates the essentially Gaussian nature of our fit results in the physical region, and the right-side axis of Figure 2 shows purely statistical significances based on Gaussian coverage. Incorporating the relatively small systematic uncertainties as a scaling factor on the change in log likelihood, the significance in the low q^2 region that $A_I^{K^{(*)}}$ is different from zero is 3.2σ for $K\ell^+\ell^-$ and 2.7σ for $K^*\ell^+\ell^-$. We have verified these confidence intervals by performing fits to ensembles of simulated datasets generated with $A_I^{K^{(*)}} = 0$ fixed, and we find frequentist coverage consistent with the $\Delta \ln \mathcal{L}$ calculations. The highly negative $A_I^{K^{(*)}}$ values for both $K\ell^+\ell^-$ and $K^*\ell^+\ell^-$ at low q^2 suggest that this asymmetry may be insensitive to the hadronic final state, and so we sum the likelihood curves as shown in Figure 2 and obtain $A_I^{K^{(*)}} = -0.64^{+0.15}_{-0.14} \pm 0.03$. Including systematics, this is a 3.9σ difference from a null $A_I^{K^{(*)}}$ hypothesis.

For the angular analysis, because of the relatively small number of expected $K^*\ell^+\ell^-$ signal candidates in each q^2 region, a simultaneous fit over $m_{\rm ES}$, $\cos\theta_K$ and $\cos\theta_\ell$ is not possible, and an iterated fitting procedure is used. The first step is an $m_{\rm ES}$ fit, with the same underlying components as above, in each q^2 region for total signal (N_S) and combinatoric background (N_B) yields for the combination of all $K^*\ell^+\ell^-$ final states. The second fit is to $\cos\theta_K$ for events with $m_{\rm ES} > 5.27\,{\rm GeV}/c^2$, where the only free parameter is F_L, and normalizations for signal and combinatorial background events are taken from the initial $m_{\rm ES}$ fit. The background normalization is obtained by integrating, for $m_{\rm ES} > 5.27\,{\rm GeV}/c^2$, the ARGUS shape resulting from the $m_{\rm ES}$ fit. We model the $\cos\theta_K$ shape of the combinatorial background using e^+e^- and $\mu^+\mu^-$ events, as well as lepton-flavor violating $e^+\mu^-$ and μ^+e^- events, in the $5.20 < m_{\rm ES} < 5.27\,{\rm GeV}/c^2$ sideband. Simulated events are used to account for the small remaining background

Table I: $A_I^{K^{(*)}}$ results. Errors are statistical and systematic, respectively.

Mode	low q^2	high q^2
$B \to K\mu^+\mu^-$	$-0.91^{+1.2}_{-\infty} \pm 0.18$	$0.39^{+0.35}_{-0.46} \pm 0.04$
$B \to Ke^+e^-$	$-1.41^{+0.49}_{-0.69} \pm 0.04$	$0.21^{+0.32}_{-0.41} \pm 0.03$
$B \to K\ell^+\ell^-$	$-1.43^{+0.56}_{-0.85} \pm 0.05$	$0.28^{+0.24}_{-0.30} \pm 0.03$
$B \to K^*\mu^+\mu^-$	$-0.26^{+0.50}_{-0.34} \pm 0.05$	$-0.08^{+0.37}_{-0.27} \pm 0.05$
$B \to K^*e^+e^-$	$-0.66^{+0.19}_{-0.17} \pm 0.02$	$0.32^{+0.75}_{-0.45} \pm 0.03$
$B \to K^*\ell^+\ell^-$	$-0.56^{+0.17}_{-0.15} \pm 0.03$	$0.18^{+0.36}_{-0.28} \pm 0.04$

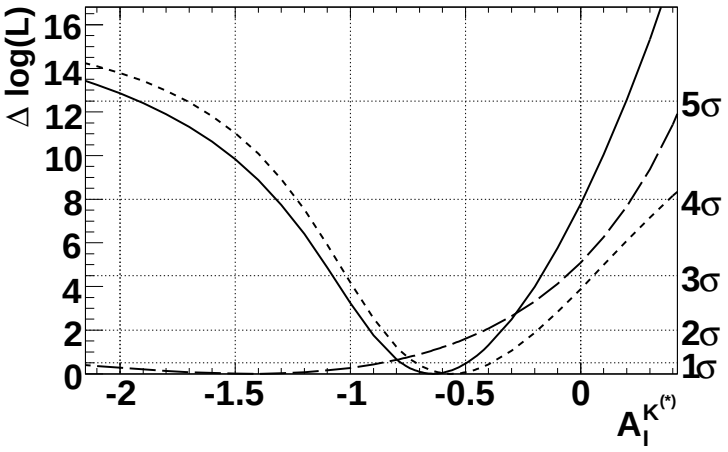

Figure 2: Low q^2 region $A_I^{K^{(*)}}$ fit likelihood curves. $K\ell^+\ell^-$ [long dash], $K^*\ell^+\ell^-$ [short dash], $(K, K^*)\ell^+\ell^-$ [solid].

contributions. The signal distribution given in Eq. 2 is folded with a model for the signal acceptance as a function of $\cos\theta_K$ obtained from simulated signal events.

The final fit is to $\cos\theta_\ell$, again for events with $m_{\rm ES} > 5.27\,{\rm GeV}/c^2$, where the only free parameter is $\mathcal{A}_{FB}$. This fit requires the value of F_L as an input, which is taken from the second fit, as are the normalizations for signal and combinatorial background. The $\cos\theta_\ell$ shape of the combinatorial background is obtained using the same sideband samples as for the $\cos\theta_K$ fit. Correlated leptons coming from $B \to D^{(*)}\ell\nu$, $D \to K^{(*)}\ell\nu$ give rise to a peak in the combinatorial background at $\cos\theta_\ell > 0.7$ which varies as a function of $m_{\rm ES}$, and we consider this variation in our study of systematic uncertainties. As for $\cos\theta_\ell$, the signal distribution given in Eq. 3 is folded with a model of signal acceptance as a function of $\cos\theta_\ell$ taken from simulated events. We again test our fits using the large sample of vetoed charmonium events, where $\mathcal{A}_{FB}$ is expected to be zero, and branching fractions and the K^* polarization are well-known [19, 20], and obtain results consistent with accepted values for each of the six individual $K^*\ell^+\ell^-$ final states, as well as their combination. We further test our methodology by performing the $m_{\rm ES}$ and $\cos\theta_\ell$ fits on a $B^+ \to K^+\ell^+\ell^-$ sample, where $\mathcal{A}_{FB} \sim 0$ is expected in most new physics models as well as the SM, and find values consistent with a null result in both low and high q^2 regions.

We consider systematic effects from several sources. Uncertainties in yields due to variations in the ARGUS shape in the $m_{\rm ES}$ fits are propagated into both angular fits, and uncertainties on the fit F_L values are propagated into the $\mathcal{A}_{FB}$ fits. Combinatorial background angular shapes are varied by dividing the sideband sample into two disjoint regions in $m_{\rm ES}$. We vary the signal model using simulated events generated with different form factors [12, 21] and a wide range of values of C_7, C_9 and C_{10}. We perform fits to large ensembles of datasets for each generator variation to determine an average absolute fit bias. Finally, we constrain the modeling of mis-reconstructed signal events from the fits to the charmonium samples, where it is the largest systematic uncertainty. As with $A_I^{K^{(*)}}$, the final systematic uncertainties are small compared to the statistical ones.

The results for F_L and $\mathcal{A}_{FB}$ are shown in Fig. 1. In the low q^2 region, where we expect $\mathcal{A}_{FB} = -0.03 \pm 0.01$ [22] and $F_L = 0.63 \pm 0.03$ [10] from the SM, we measure $\mathcal{A}_{FB} = 0.24^{+0.18}_{-0.23} \pm 0.05$ and $F_L = 0.35 \pm 0.16 \pm 0.04$, where the first error is statistical and the second is systematic. In the high q^2 region, the SM expectation is $\mathcal{A}_{FB} \sim 0.26$ and $F_L \sim 0.40$, and we measure $\mathcal{A}_{FB} = 0.76^{+0.52}_{-0.32} \pm 0.07$ and $F_L = 0.71^{+0.20}_{-0.22} \pm 0.04$, with a signal yield of 36.6 ± 9.6 events. Theoretical uncertainties on the expected SM F_L and $\mathcal{A}_{FB}$ values in the high q^2 region are difficult to characterize, and the quoted values are obtained from our signal event generator [12, 21].

The magnitude of possible contributions from new physics to C_{10} can be constrained by a positive sign of $\mathcal{A}_{FB}$ at high q^2. By combining $\mathcal{A}_{FB}$ with inclusive branching fraction results, an upper bound of $|C_{10}^{NP}| <\sim 7$ can be obtained, improving on an upper bound derived solely from branching fraction results of $|C_{10}^{NP}| <\sim 10$ [23]. The $\mathcal{A}_{FB}$ results additionally exclude a wrong-sign $C_9 C_{10}$ from purely right-handed weak currents at more than 3 standard deviations significance. The low q^2 AFB result suggests that a zero-crossing point, a distinctive SM feature, may not be present. Some angular asymmetries in the K^* system include the longitudinal polarization as a component and are more sensitive to possible new physics contributions than measurements of F_L alone, as predicted values for these asymmetries in the SM and various new physics models can be calculated with relatively small theory uncertainties [24]. However, such asymmetries could not be considered here as they require analysis of a dataset substantially greater than currently available. Our results are consistent with measurements by Belle [25], and replace the earlier *BABAR* results in which only a lower limit on $\mathcal{A}_{FB}$ was set in the low q^2 region [5].

References

[1] G. Buchalla, A. J. Buras and M. E. Lautenbacher, Rev. Mod. Phys. **68**, 1125 (1996).

[2] A. Ali, E. Lunghi, C. Greub and G. Hiller, Phys. Rev. D **66**, 034002 (2002).

[3] G. Burdman, Phys. Rev. D **52**, 6400 (1995); J. L. Hewett and J. D. Wells, Phys. Rev. D **55**, 5549 (1997); Q. S. Yan, C. S. Huang, W. Liao and S. H. Zhu, Phys. Rev. D **62**, 094023 (2000); T. Feldmann and J. Matias, JHEP **0301**, 074 (2003); W. J. Li, Y. B. Dai and C. S. Huang, Eur. Phys. J. C **40**, 565 (2005); Y. G. Xu, R. M. Wang and Y. D. Yang, Phys. Rev. D **74**, 114019 (2006); P. Colangelo, F. De Fazio, R. Ferrandes and T. N. Pham, Phys. Rev. D **73**, 115006 (2006).

[4] F. Kruger, L. M. Sehgal, N. Sinha and R. Sinha, Phys. Rev. D **61**, 114028 (2000) [Erratum-ibid. D **63**, 019901 (2001)].

[5] B. Aubert *et al.* [*BABAR* Collaboration], Phys. Rev. D **73**, 092001 (2006).

[6] Heavy Flavor Averaging Group, E. Barberio *et al.*, arXiv:0704.3575 (2007).

[7] T. Feldmann and J. Matias, JHEP **0301**, 074 (2003).

[8] M. Beneke, T. Feldmann and D. Seidel Eur. Phys. J. **C41**, 173 (2005).

[9] T. Feldmann, 5th Workshop on the CKM Unitary Triangle, Rome (2008).

[10] F. Kruger and J. Matias, Phys. Rev. D **71**, 094009 (2005).

[11] A. Ali, P. Ball, L. T. Handoko and G. Hiller, Phys. Rev. D **61**, 074024 (2000)

[12] F. Kruger, L. M. Sehgal, N. Sinha and R. Sinha, Phys. Rev. D **61**, 114028 (2000) [Erratum-ibid. D **63**, 019901 (2001)]; A. Ali, E. Lunghi, C. Greub and G. Hiller, Phys. Rev. D **66**, 034002 (2002); K. S. M. Lee, Z. Ligeti, I. W. Stewart and F. J. Tackmann, Phys. Rev. D **75**, 034016 (2007).

[13] M. Beneke, T. Feldmann and D. Seidel, Nucl. Phys. B **612**, 25 (2001);

[14] C. Bobeth, M. Bona, A. J. Buras, T. Ewerth, M. Pierini, L. Silvestrini and A. Weiler, Nucl. Phys. B **726**, 252 (2005).

[15] A. Hovhannisyan, W. S. Hou and N. Mahajan, Phys. Rev. D **77**, 014016 (2008).

[16] B. Aubert *et al.* [BABAR Collaboration], Nucl. Instrum. Meth. A **479**, 1 (2002).

[17] W. M. Yao *et al.* [Particle Data Group], J. Phys. G **33** (2006) 1.

[18] H. Albrecht *et al.* [ARGUS Collaboration], Z. Phys. C **48**, 543 (1990).

[19] W. M. Yao *et al.* [Particle Data Group], J. Phys. G **33** (2006) 1.

[20] B. Aubert *et al.* [BABAR Collaboration], Phys. Rev. D **76**, 031102 (2007).

[21] P. Ball and R. Zwicky, Phys. Rev. D **71**, 014029 (2005).
[22] T. Huber, T. Hurth and E. Lunghi, arXiv:0712.3009 [hep-ph], submitted to Nucl.Phys.B.
[23] C. Bobeth, G. Hiller and G. Piranishvili, JHEP **0807**, 106 (2008) [arXiv:0805.2525 [hep-ph]].
[24] E. Lunghi and J. Matias, JHEP **0704**, 058 (2007)
[25] A. Ishikawa *et al.*, Phys. Rev. Lett. **96**, 251801 (2006).